Steady-state Fluorescence Emission Studies on Polyazacyclophane Macrocyclic Receptors and on their Adducts with Hexacyanocobaltate(III)

Mª. Alexandra Bernardo,[a] A. Jorge Parola,[a] Fernando Pina,*[,a] Enrique Garcia-España,*[,b] Victor Marcelino,[b] Santiago V. Luis*[,c] and Juan F. Miravet[c]

[a] *Departamento de Química da Faculdade de Ciências e Tecnologia da Universidade Nova de Lisboa, Monte de Caparica, Portugal*

[b] *Departament de Química Inorgànica, Facultat de Química, Universitat de València, C/Dr. Moliner 50, 46100 Burjassot (València), Spain*

[c] *Departamento de Ciencias Experimentales, Laboratorio de Química Orgánica, Universitat Jaume I (Castellón), Spain*

The steady-state fluorescence emission spectra of the azacyclophanes 2,5,8,11-tetraaza[12]paracyclophane (L^1), 2,6,9,13-tetraaza[14]paracyclophane (L^2), 14,15,17,18-tetramethyl-2,5,8,11-tetraaza[12]paracyclophane (L^3) and 16,17,19,20-tetramethyl-2,6,9,13-tetraaza[14]paracyclophane (L^4) as a function of pH have been measured. The fully protonated species of each cyclophane gives the highest fluorescence-emission quantum yield. The shapes of the titration curves have been explained by the existence of an electron-transfer quenching effect from a non-protonated amine to the benzene chromophore. This effect is greater for macrocycles in which the first deprotonated amine group is closer to the benzene. The association constants for the interaction of the four fully protonated macrocycles with $K_3[Co(CN)_6]$ have been measured either by potentiometry or from fluorescence-emission measurements, and increase in the order $L^3 \approx L^4 < L^1 \approx L^2$. The photoaquation quantum yields of $K_3[Co(CN)_6]$ have been measured in the presence of the macrocycles L^1 and L^2, and indicate that three of the CN nitrogens of the complex are involved in adduct formation with the fully protonated macrocycles, as supported by molecular modelling.

Supramolecular interactions between protonated cyclic polyamines and negatively charged cyano complexes *via* electrostatic interactions and/or hydrogen bonds, have been described in recent years.[1-3] The most studied adducts are those formed between $[Co(CN)_6]^{3-}$ and a series of cyclic polyamines possessing different dimensions and charge. The formation of the adducts does not affect the nature of the photoreaction of the co-ordination compound but decreases the respective quantum yield to a third, a half or two thirds. These results were interpreted as an effect of the hydrogen bonding between the protonated nitrogens of the macrocycle and the nitrogens of the cyanide ligand, which prevents CN^- from escaping out of the first co-ordination sphere. The dimensions of the macrocyclic receptor are crucial. Reduction to a third was observed exclusively for the octaprotonated form of 1,5,9,13,17,21,25,29-octaazacyclodotriacontane ([32]aneN_8), suggesting in this case that four out of the six CN^- groups in $[Co(CN)_6]^{3-}$ are involved in the hydrogen-bond network with the receptor. Other smaller polyammonium receptors such as the fully N-protonated forms of 1,4,7,10,13,16,19,22-octaazacyclotetracosane ([24]aneN_8), 1,5,9,13,17,21-hexaazacyclotetracosane ([24]aneN_6) and 1,4,7,10,13,16,19,22,25,28-decaazacyclotriacontane ([30]aneN_{10}) reduced the photoreaction quantum yield by a half,[1,2] a result compatible with the participation of three CN^- groups in hydrogen bonding. The analogous open-chain receptor 1,19-diamino-4,8,12,16-tetraazanonadecane reduces the aquation quantum yield to two thirds, which indicates the presence of only two hydrogen bonds. More recently it was demonstrated that for open-chain branched poly(ethyleneimine) polymers, no more than four cyanide ligands per complex are bound to the polymer.[4]

Recently,[5,6] the protonation behaviour of a series of cyclophanes containing a *para*-substituted benzene or durene (1,2,4,5-tetramethylbenzene) spacer interrupting polyamine chains with different numbers of nitrogen atoms and sequences of hydrocarbon chains has been studied. The protonation behaviour of these compounds[7,8] suggested their possible use for anion co-ordination studies as they accumulate high positive charge in aqueous solution. Here we report on the potentiometric determination of the interaction constants with hexacyanocobaltate(III) of the receptors 2,5,8,11-tetraaza[12]paracyclophane (L^1), 2,6,9,13-tetraaza[14]paracyclophane-(L^2)-14,15,-17,18-tetramethy-2,5,8,11-tetraaza[12]paracyclophane (L^3) and 16,17,19,20-tetramethyl-2,6,9,13-tetraaza[14]paracyclophane (L^4).

In addition, it is interesting to perform photochemical studies on these adducts, because in contrast to polyamine receptors they exhibit fluorescence at room temperature. Moreover, the pH dependence of both UV/VIS absorption and steady-state fluorescence emission can be a useful tool for complementing the potentiometric determination of the basicity constants of the polyazacyclophanes, as well as the formation constants of the adducts with some anionic complexes.

Experimental

Materials.—Ligands L^1–L^4 were synthesised as described previously[4,5] and handled as their hydroperchlorate salts. The $NaClO_4$ used to keep the ionic strength constant was purified according to ref. 9. All the measurements, unless otherwise stated, were carried out in 0.15 mol dm^{-3} $NaClO_4$. Carbon dioxide-free NaOH solutions and HCl, or $HClO_4$ solutions were prepared following the procedure reported in ref. 10. Hexacyanocobaltate(III) was purchased from Aldrich and recrystallized twice from water–methanol mixtures.

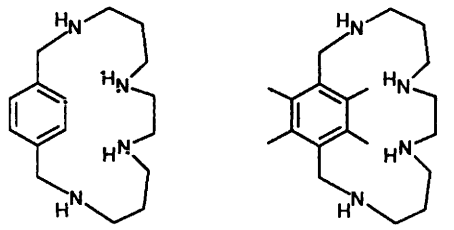

L^2 L^4

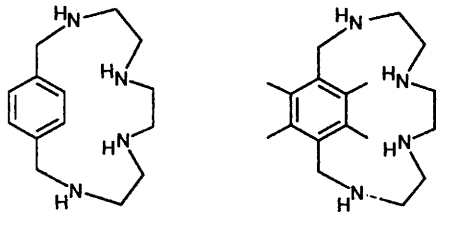

L^1 L^3

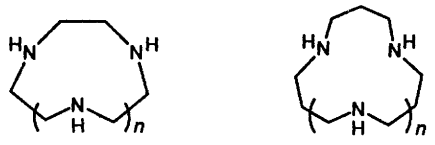

n	n
6 [24]aneN$_8$	4 [24]aneN$_6$
7 [27]aneN$_9$	6 [32]aneN$_8$
8 [30]aneN$_{10}$	

Spectrophotometric Titrations—Perchloric acid and NaOH were used to adjust the pH. Absorption spectra were recorded on a Perkin-Elmer Lambda 6 spectrophotometer and fluorescence emission spectra on a SPEX F111 Fluorolog spectrofluorimeter.

Fluorescence Quantum Yields.—Benzene was used as standard ($\Phi_0 = 0.07$ in cyclohexane)[11] for L^1 and L^2, while naphth-2-ol ($\Phi_0 = 0.32$ in cyclohexane)[11] was the standard for L^3 and L^4. For all four macrocycles the solvent used was water and the pH was maintained at 1.7 where they are fully protonated.

Fluorescence Quenching Studies.—The pH values were chosen for each macrocycle such that only the fully protonated form existed in solution.

Irradiation Experiments.—Irradiations at 313 nm (Oriel filters) were made on a xenon–mercury medium pressure lamp (PTI model A1010). The intensity of incident light was 3.5×10^{-7} Einstein min^{-1} (≈ 44.5 W m^{-2}) as measured by iron(III) oxalate actinometry.[12] Concentrations of $K_3[Co(CN)_6]$ were about 10^{-3} mol dm^{-3}. An excess of L^2 was used in order to obtain at least 90% association, while the L^1 concentration was calculated to give about 50% association owing to solubility problems. The pH values were selected such that only the fully protonated forms of the macrocycles exist in solution.

Electromotive Force Measurements.—The potentiometric titrations were carried out in 0.15 mol dm^{-3} solutions at 298.1 ± 0.1 K, by using the equipment (potentiometer, burette, stirrer, microcomputer, *etc.*) described previously.[13] The acquisition of the electromotive force (e.m.f.) data was performed using the computer program PASAT.[14] The reference electrode was an Ag–AgCl electrode in saturated KCl solution. The glass electrode was calibrated as a hydrogen concentration probe by titrating known amounts of HCl with CO_2-free NaOH solutions and determining the equivalence point by Gran's method,[15] which gives the standard potential of the electrode, $E^{o\prime}$, and the ionic product of water. The computer program SUPERQUAD[16] was employed to calculate the protonation and stability constants and the DISPO[17] program was used to obtain the distribution diagrams. At least three titration curves were performed for each one of the studied systems (*ca.* 100 experimental points). Concentrations of $[Co(CN)_6]^{3-}$ were *ca.* 2×10^{-3} mol dm^{-3} and those of the ligands varied in the range 1×10^{-3}–10^{-2} mol dm^{-3}, the pH range investigated was 2.5–10.0. Formation of anion adducts usually occurred below pH 6. The titration curves for each system were treated either as a single set or separately without significant variations in the values of the equilibrium constants. Furthermore, the sets of data were merged together to obtain the final values of the stability constants.

Results and Discussion

Absorption Measurements.—The polyazacyclophanes L^1–L^4 are involved in acid–base ground-state equilibria, equations (1)–(4), in which K_i is the acidity constant for the i^{th} equilibrium.

$$H_4L^{4+} + H_2O \rightleftharpoons H_3L^{3+} + H_3O^+ \quad (1)$$

$$H_3L^{3+} + H_2O \rightleftharpoons H_2L^{2+} + H_3O^+ \quad (2)$$

$$H_2L^{2+} + H_2O \rightleftharpoons HL^+ + H_3O^+ \quad (3)$$

$$HL^+ + H_2O \rightleftharpoons L + H_3O^+ \quad (4)$$

The absorbance A divided by the absorption of the totally protonated form A_0 obtained at sufficiently acidic pH, is described by equation (5), where $\varepsilon_{H_nL^{n+}}$ is the molar absorption coefficient for the H_nL^{n+} species, and $\gamma_{H_nL^{n+}}$ their respective

$$\frac{A}{A_0} = \gamma_{H_4L^{4+}} + \frac{\varepsilon_{H_3L}}{\varepsilon_{H_4L^{4+}}}\gamma_{H_3L^{3+}} + \frac{\varepsilon_{H_2L^{2+}}}{\varepsilon_{H_4L^{4+}}}\gamma_{H_2L^{2+}} + \frac{\varepsilon_{HL^+}}{\varepsilon_{H_4L^{4+}}}\gamma_{HL^+} + \frac{\varepsilon_L}{\varepsilon_{H_4L^{4+}}}\gamma_L \quad (5)$$

molar fractions defined according to equations (6)–(10), where K_1–K_4 are the acidity constants associated with equilibria (1)–(4).

$$\gamma_{H_4L^{4+}} = \frac{[H^+]^4}{[H^+]^4 + K_1[H^+]^3 + K_1K_2[H^+]^2 + K_1K_2K_3[H^+] + K_1K_2K_3K_4} \quad (6)$$

$$\gamma_{H_3L^{3+}} = \frac{K_1[H^+]^3}{[H^+]^4 + K_1[H^+]^3 + K_1K_2[H^+]^2 + K_1K_2K_3[H^+] + K_1K_2K_3K_4} \quad (7)$$

$$\gamma_{H_2L^{2+}} = \frac{K_1K_2[H^+]^2}{[H^+]^4 + K_1[H^+]^3 + K_1K_2[H^+]^2 + K_1K_2K_3[H^+] + K_1K_2K_3K_4} \quad (8)$$

$$\gamma_{HL^+} = \frac{K_1K_2K_3[H^+]}{[H^+]^4 + K_1[H^+]^3 + K_1K_2[H^+]^2 + K_1K_2K_3[H^+] + K_1K_2K_3K_4} \quad (9)$$

$$\gamma_L = \frac{K_1K_2K_3K_4}{[H^+]^4 + K_1[H^+]^3 + K_1K_2[H^+]^2 + K_1K_2K_3[H^+] + K_1K_2K_3K_4} \quad (10)$$

Table 1 The pK_a values for the receptors L^1–L^4 and data obtained from the fitting of equations (5) and (11)[a]

	L^1	L^2	L^3[b]	L^4
pK_{a1}	2.51(1),[c] 2.2,[d,e] 2.25(5)[f]	3.61(1),[c] 3.5(1)[f]	2.5(1)[c]	3.59(3),[c] 3.1(1),[d] 3.1[e,f]
pK_{a2}	5.58(2),[c] 5.3(1),[d] 5.6(1)[f]	7.43(1),[c] 7.4(1),[d] 7.4(1)[f]	5.64(6),[c] 5.3(1)[d]	7.44(2),[c] 7.5(1),[d] 7.1(1)[f]
pK_{a3}	8.45(2),[c] 8.5[d,e]	9.09(1),[c] 9.1[e,f]	8.67(3),[c] 8.7(1)[d]	9.23(2),[c] 9.2,[d,e] 9.2[e,f]
pK_{a4}	9.39(2)[c]	9.933(4)[c]	9.44(3),[c] 9.5(1)[d]	10.54(1),[c] 10.6(1),[d] 10.6[e,f]
$\varepsilon_{H_3L^{3+}}/\varepsilon_{H_4L^{4+}}$	1.1[d]	1[d]	0.96[d]	1.02[d]
$\varepsilon_{H_2L^{2+}}/\varepsilon_{H_4L^{4+}}$	0.6[d]	0.6[d]	0.56[d]	0.8[d]
$\varepsilon_{HL^{+}}/\varepsilon_{H_4L^{4+}}$	0.5[d]	0.6[d]	0.3[d]	0.7[d]
$\varepsilon_{L}/\varepsilon_{H_4L^{4+}}$	0.5[d]	0.6[d]	0.18[d]	0.6[d]
$\varphi_{H_3L^{3+}}/\varphi_{H_4L^{4+}}$	0.16[f]	0.55[f]	—	0.59[f]
$\varphi_{H_2L^{2+}}/\varphi_{H_4L^{4+}}$	—	0.06[f]	—	0.19[f]
$\varphi_{HL^{+}}/\varphi_{H_4L^{4+}}$	—	—	—	0.13[f]
$\varphi_{L}/\varphi_{H_4L^{4+}}$	—	—	—	—

[a] Values in parentheses are standard deviations on the last significant figure. [b] Quantum yield for fluorescence emission too low for quantitative measurements. [c] Values calculated by potentiometry (ref. 7). [d] Values obtained from UV/VIS spectroscopy [equation (5)]. [e] Values for which accuracy is not high, due to the small differences between the respective molar absorption coefficients. [f] Values obtained from fluorescence emission [equation (11)].

Equation (5) can be used to fit the titration curves followed by UV/VIS spectroscopy, using the acidity constants obtained by potentiometric titrations [from which all the $\gamma_{H_nL^{n+}}$ terms in equation (5) may be calculated] and by adjusting the four ratios $\varepsilon_{H_nL^{n+}}/\varepsilon_{H_4L^{4+}}$. In some cases, in order to obtain the best fit, it is necessary to change (generally slightly) the initial (potentiometric) acidity constants. This procedure enables the potentiometric data to be adequately standardized.

Fig. 1 shows the absorption spectra for L^1 as a function of pH and the titration curve recorded at 270 nm (absorption maximum) in 0.15 mol dm^{-3} $NaClO_4$. A similar pattern was observed for the other receptors, and the results obtained from equation (5) are shown in Table 1.

The similarities in the shape of the first singlet absorption of the macrocycle, with the respective original aromatic component (benzene or durene), suggest a π–π^* character for this transition. Inspection of Table 1 shows the limitations of this method to evaluate acidity constants. Sensitivity is dependent upon the difference between the consecutive molar absorption coefficients: *e.g.*, for L^1 and L^2, only $\varepsilon_{H_2L^{2+}}$ and $\varepsilon_{H_3L^{3+}}$ are sufficiently different to obtain a good accuracy.

Steady-state Fluorescence Emission.—Where no excited-state acid–base equilibria is observed, the titration curves obtained by steady-state fluorescence emission are given by equation (11), where I is the fluorescence-emission intensity for a given

$$\frac{I}{I_0} = \gamma_{H_4L^{4+}} + \frac{\varphi_{H_3L^{3+}}}{\varphi_{H_4L^{4+}}}\gamma_{H_3L^{3+}} + \frac{\varphi_{H_2L^{2+}}}{\varphi_{H_4L^{4+}}}\gamma_{H_2L^{2+}} + \frac{\varphi_{HL^{+}}}{\varphi_{H_4L^{4+}}}\gamma_{HL^{+}} + \frac{\varphi_{L}}{\varphi_{H_4L^{4+}}}\gamma_{L} \quad (11)$$

pH value, and I_0 is the fluorescence maximum intensity obtained at the first plateau, which corresponds to the fluorescence-emission maximum of the totally protonated form, and $\varphi_{H_nL^{n+}}$ are the fluorescence emission quantum yields for the H_nL^{n+} species. Equation (11) can be used to fit the experimental data. The steady-state fluorescence emission spectra and the respective titration curves for L^1 and L^2 are depicted in Figs. 2 and 3, respectively and the data obtained from the fitting of the equation are given in Table 1.

We did not observe inflections on these curves which could be attributed to acid–base equilibria in the excited state and therefore all the observed inflections are due to ground-state acid–base properties. This is in agreement with the absence of changes in the position of both absorption and emission maxima of the main emitting species H_4L^{4+} and H_3L^{3+} and, in effect, as noted by Förster,[18] the acidity constant of the excited-state species, pK_a^*, is equal to pK_a. In other words the lifetime of the species is lower than the deprotonation and protonation rate constants in the excited state. Accordingly, equation (11) can be used to calculate the acidity constants as well as the ratio between the fluorescence-emission quantum yields. As in the titration curves obtained by UV/VIS spectroscopy the acidity constants obtained by potentiometry were used as the starting point for the fitting, the best fit was achieved with small changes in these constants. One main feature that emerges from these curves is the much higher fluorescence-emission quantum yield of the totally protonated macrocycle. In all the macrocycles, removal of the first proton from N^6 (or N^9 in L^2 and L^4) or N^5 (or N^8 in L^1 and L^3) of the totally protonated species gives rise to a large decrease in the fluorescence-emission quantum yield. Owing to the chemical structure of the molecule, the benzene ring is expected to be not only the chromophore but also the fluorophore. It is well known that amines are able to transfer electrons to the excited benzene,[19–24] giving rise to a quenching effect on the fluorescence emission of the first singlet state of benzene. When amines are protonated they are not efficient quenchers owing to the effect of the positive charge. Deprotonation of the first nitrogen in the macrocycle results in the initiation of this internal quenching phenomena. As this is dependent on the electron-transfer distance, the smallest macrocycle shows the largest effect on deprotonation.

From the fluorescence-emission quantum yields of the fully protonated forms of the four macrocycles (see Table 2), the largest values are observed for the benzene derivatives and, in

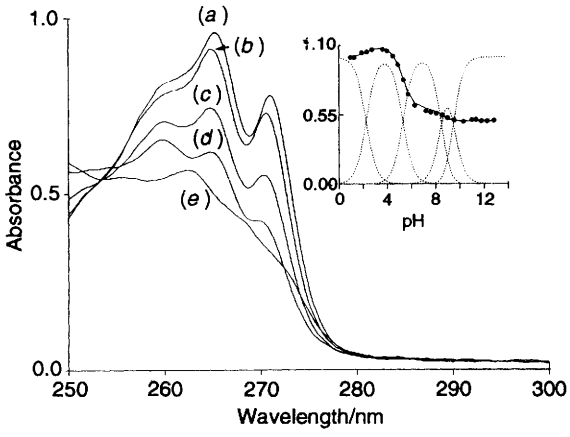

Fig. 1 Absorption spectra of L^1 as a function of pH: (*a*) pH 1.6, (*b*) 3.92, (*c*) 5.25, (*d*) 7.45, (*e*) 12.1; ionic strength 0.15 mol dm^{-3} $NaClO_4$. Inset: (· · · ·) distribution diagram calculated from the potentiometric constants; (●) normalized absorption at 270 nm; (——) fitting curve

the same family, the largest fluorescence quantum yields correspond to the macrocycles with the largest cavity sizes.

Determination of the Association Constants by Steady-state Fluorescence Emission.—Two different mechanisms may be observed on the fluorescence-emission quenching of the species, H_nL^{n+}, by a quencher, Q, as is shown in equations (12)–(15).

$$H_nL^{n+} \xrightarrow{h\nu} H_nL^{n+}* \quad (12)$$

$$H_nL^{n+}* + Q \xrightarrow{k_q} H_nL^{n+} \quad (13)$$

$$H_nL^{n+} + Q \rightleftharpoons H_nL^{n+}\cdot Q \quad (14)$$

$$H_nL^{n+}\cdot Q \xrightarrow{h\nu} \text{complete quenching} \quad (15)$$

According to equation (13) the excited species must be diffused in order to encounter a molecule of Q prior to deactivation, giving rise to the well known Stern–Volmer kinetics.[25] Another possible route to quenching is the existence of a ground-state association between H_nL^{n+} and Q. It is possible to distinguish the two types of quenching by equation (16), where

$$[(I_0 - I)/I]/[Q] = K' + K_q\tau_0 + K'K_q\tau_0[Q] \quad (16)$$

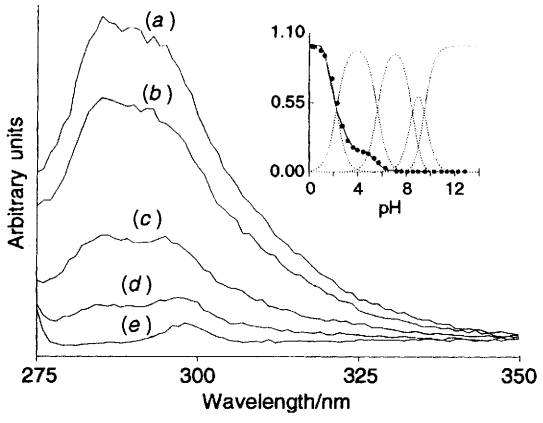

Fig. 2 Emission spectra of L^1 as a function of pH: (*a*) pH 1.3, (*b*) 1.9, (*c*) 3.18, (*d*) 5.33, (*e*) 11.0; ionic strength 0.15 mol dm^{-3} $NaClO_4$. Inset: (· · ·) distribution diagram calculated from the potentiometric constants; (●) normalized absorption at 284 nm; (——) fitting curve

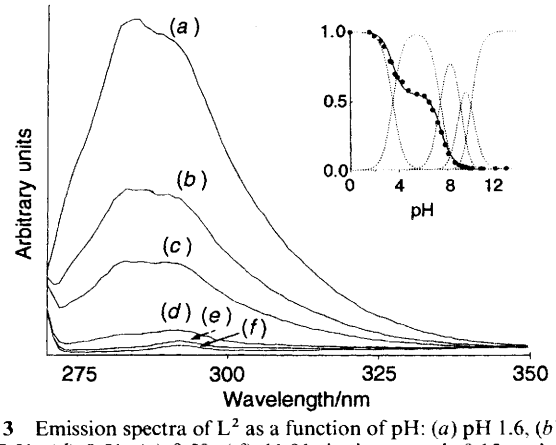

Fig. 3 Emission spectra of L^2 as a function of pH: (*a*) pH 1.6, (*b*) 6.5, (*c*) 7.51, (*d*) 8.51, (*e*) 9.50, (*f*) 11.91; ionic strength 0.15 mol dm^{-3} $NaClO_4$. Inset: (· · ·) distribution diagram calculated from the potentiometric constants; (●) normalized absorption at 285 nm; (——) fitting curve

$K' = K_f(\varepsilon_{H_nL^{n+}\cdot Q}/\varepsilon_{H_nL^{n+}})$ and $\varepsilon_{H_nL^{n+}\cdot Q}$ and $\varepsilon_{H_nL^{n+}}$ are respectively the molar absorptivities of the complex and emissive species at the excitation wavelength, and τ_0 the decay lifetime of the emissive species in the absence of quencher.

When the emission lifetime is low and the association constant relatively high, equation (16) is simplified to equation (17), from which it is possible to calculate the association constants.

$$K_f = \frac{(I_0 - I)\varepsilon_{H_nL^{n+}}}{I[Q]\varepsilon_{H_nL^{n+}\cdot Q}} \quad (17)$$

The emission of the fully protonated forms of the four macrocycles was followed as a function of the added concentration of hexacyanocobaltate(III) in 0.15 mol dm^{-3} $NaClO_4$. Equation (17) was verified for all the adducts, which means that no dynamic quenching was observed, and only total quenching of the ground-state adduct is operative. The results are reported in Table 3.

We have verified that adduct formation does not affect the absorption spectra, which are identical to the addition spectra of the two components, as expected for partners not giving low-energy charge-transfer transitions. Inspection of Table 3 clearly shows that the largest association constants are obtained for the benzene derivatives. Their durene analogs possess four methyl groups which may hinder the approach of the complex.

Photoaquation Quantum Yields.—Irradiation of hexacyanocobaltate(III) at 313 nm was performed in the presence of the macrocycles L^1 and L^2 at pH 1.7. In both cases it is not possible to use large amounts of macrocycle due to problems of solubility, and with the compound L^4 no sufficient solubility of the adduct was achieved to carry out the experiments. The photochemical experiments were measured without any addition of salts to maintain the ionic strength, because this would increase the association constant. Corrections were made for the amount of adduct associated. The photoaquation quantum yields obtained were 0.30 for $K_3[Co(CN)_6]$ with no receptor present, and 0.14 and 0.16 for this complex in the presence of L^1 and L^2 respectively. This reduction by a factor of two for the quantum yield observed for both adducts can be interpreted by assuming that three out of the six cyanides of hexacyanocobaltate(III) are involved in hydrogen bonding with the adduct.

Table 2 Fluorescence quantum yields (φ_F) at pH 1.7*

Receptor	φ_F
L^1	0.02
L^2	0.07
L^3	0.002
L^4	0.006

* Estimated errors of ± 15%.

Table 3 Association constants (in log units) of the adducts formed between hexacyanocobaltate(III) and the H_4L^{4+} forms of the macrocyclic receptors L^1–L^4 determined by potentiometry at 298.1 K in 0.15 mol dm^{-3} $NaClO_4$ and by quenching of the steady-state fluorescence emission*

	Method	
Receptor	Potentiometry	Emission
L^1	3.42(2)	3.5(1)
L^2	3.59(2)	3.5(1)
L^3	3.12(2)	3.0(1)
L^4	3.0(1)	2.9(1)

* Values in parentheses are standard deviations on the last significant figure.

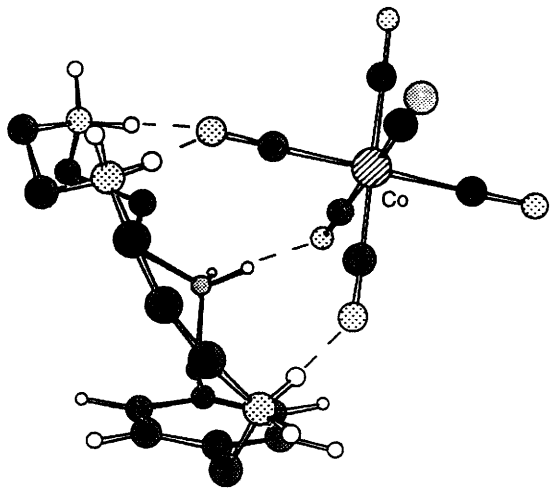

Fig. 4 Schematic representation of the interaction of $[Co(CN)_6]^{3-}$ and $[H_4L^2]^{4+}$ showing the formation of hydrogen bonds

Conclusion

Association constants for the receptors L^1–L^4 clearly show that for those pairs of ligands with the same polyamine bridge, L^1 and L^3, or L^2 and L^4, the receptors containing benzene as spacer display significantly larger interaction constants than those with durene (see Table 3). However, for ligands with the same spacer, changes in the length of the hydrocarbon chains between the nitrogen atoms do not seem to have a great effect on the strength of the interaction. These results suggest that the introduction of the methyl groups in the aromatic spacer somehow hinders the approach of the $[Co(CN)_6]^{3-}$ anion. In fact Corey–Pauling–Koltun (CPK) models show that the polyamine bridge is arching above the aromatic moiety and consequently the methyl groups are directed towards both sides of the macrocyclic cavity. Thus the matching between host and guest species which dictates the hydrogen-bond network should be more difficult in durene-containing paraazacyclophanes.

Photochemical results suggest that three out of the six cyanide groups of the anion are participating in the formation of hydrogen bonds with the receptor. Again, CPK models are useful in this respect, since due to the remarkable rigidity of the receptors, they show that for geometric reasons only three facial cyanide groups may interact with the protonated nitrogens of the macrocyclic framework (see Fig. 4). We are currently carrying out further molecular-modelling studies to understand better the different energetic contributions affecting these interactions.

Comparison of these results with previous values found in the literature[1–3] is difficult owing to the differences in topology between these polyazacyclophanes and the large polyammonium compounds that, to date, have been usually tested as $[Co(CN)_6]^{3-}$ hosts. However, while the order of magnitude of the association constants between the tetraprotonated receptors $[H_4L^1]^{4+}$ and $[H_4L^2]^{4+}$ and $[Co(CN)_6]^{3-}$ is greater than those values obtained for larger polyazacycloalkanes with the same degree of protonation, the cyclophanes with a durene spacer have similar association constants to the polyazacycloalkanes {for instance for L = [27]aneN$_9$ (1,4,7,10,13,16,19,22,25-nonaazacycloheptacosane), $H_4L^{4+} + [Co(CN)_6]^{3-} \rightleftharpoons H_4L[Co(CN)_6]^+$, $\log K = 2.61$, $H_6L^{6+} + [Co(CN)_6]^{3-} \rightleftharpoons H_4L[Co(CN)_6]^{3+}$, $\log K = 3.36$; for [30]aneN$_{10}$ (1,4,7,10,13,16,19,22,25,28-decaazacyclotriacontane), $H_4L^{4+} + [Co(CN)_6]^{3-} \rightleftharpoons H_4L[Co(CN)_6]^+$, $\log K = 2.03$, $H_6L^{6+} + [Co(CN)_6]^{3-} \rightleftharpoons H_4L[Co(CN)_6]^{3+}$, $\log K = 2.37$; for [33]aneN$_{11}$ (1,4,7,10,13,16,19,22,25,28,31-undecaazacyclotritriacontane), $H_4L^{4+} + [Co(CN)_6]^{3-} \rightleftharpoons H_4L[Co(CN)_6]^+$, $\log K = 2.63$, $H_6L^{6+} + [Co(CN)_6]^{3} \rightleftharpoons H_4L[Co(CN)_6]^{3+}$, $\log K = 3.52$}.[3] These values reflect the different accumulations of positive charge and matching with the guest afforded by the different receptors. For a given degree of protonation, charge density should be larger in the small paraazacyclophanes considered here than in the larger macrocycles, but the methyl groups on the aromatic moieties of L^3 and L^4 considerably hinder the approach and matching which dictate the molecular assembly through hydrogen bonds.

Acknowledgements

We are indebted to the Dirección General de Investigación Cientifica y Técnica (PB93-0700-CO2) and Portuguese Junta Nacional de Investigação Cientifica e Tecnológica (STRIDE/C/CEN/437/92) for financial support. J. F. M. thanks the Conselleria de Educación i Ciencia for a predoctoral fellowship and M. A. B. thanks the Instituto de Biologia Experimental e Tecnológica (PEDIP 2, medida no. 4, proc. 1495).

References

1 M. F. Manfrin, L. Moggi, V. Castelvetro, V. Balzani, M. W. Hosseini and J.-M. Lehn, *J. Am. Chem. Soc.*, 1985, **107**, 6888.
2 F. Pina, L. Moggi, M. F. Manfrin, V. Balzani, M. W. Hosseini and J.-M. Lehn, *Gazz. Chim. Ital.*, 1989, **119**, 65.
3 A. Bianchi, E. García-España, S. Mangani, M. Micheloni, P. Orioli and P. Paoletti, *J. Chem. Soc., Chem. Commun.*, 1987, 729; A. Bencini, A. Bianchi, E. García-España, M. Giusti, S. Mangani, M. Micheloni, P. L. Orioli and P. Paoletti, *Inorg. Chem.*, 1987, **26**, 3902.
4 M. F. Manfrin, L. Setti and L. Moggi, *Inorg. Chem.*, 1992, **31**, 2768.
5 A. Andrés, M. I. Burguete, E. García-España, S. V. Luis, J. F. Miravet and C. Soriano, *J. Chem. Soc., Perkin Trans. 2*, 1993, 749.
6 A. Bencini, M. I. Burguete, E. García-España, S. V. Luis, J. F. Miravet and C. Soriano, *J. Org. Chem.*, 1993, **58**, 4749.
7 A. Bianchi, B. Escuder, E. García-España, S. V. Luis, V. Marcelino, J. F. Miravet and J. A. Ramírez, *J. Chem. Soc., Perkin Trans. 2*, 1994, 1253.
8 A. Andrés, C. Bazzicalupi, A. Bianchi, E. García-España, S. V. Luis, J. F. Miravet and J. A. Ramírez, *J. Chem. Soc., Dalton Trans.*, 1994, 1995.
9 M. Micheloni, P. May and D. R. Williams, *J. Inorg. Nucl. Chem.*, 1978, **40**, 1209.
10 M. Micheloni, A. Sabatini and A. Vacca, *Inorg. Chim. Acta*, 1977, **25**, 41.
11 I. B. Berlman, *Handbook of Fluorescence Spectra of Aromatic Molecules*, Academic Press, New York, 1971, p. 108.
12 C. G. Hatchard and C. A. Parker, *Proc. R. Soc. London Ser. A*, 1956, **235**, 518.
13 E. García-España, M.-J. Ballester, F. Lloret, J.-M. Moratal, J. Faus and A. Bianchi, *J. Chem. Soc., Dalton Trans.*, 1988, 101.
14 M. Fontanelli and M. Micheloni, Proceedings of the First Spanish-Italian Congress on Thermodynamics of Metal Complexes, Peñíscola, Spain, June 3–6, 1990.
15 G. Gran, *Analyst (London)*, 1952, **77**, 881; F. J. Rossoti and H. Rossotti, *J. Chem. Educ.*, 1965, **42**, 375.
16 P. Gans, A. Sabatini and A. Vacca, *J. Chem. Soc., Dalton Trans.*, 1985, 1195.
17 A. Vacca, FORTRAN program to determine from the stability constants and mass balance equations distribution of the species in multiequilibria systems, University of Florence, 1977.
18 T. Förster, *Z. Electrochem.*, 1950, **54**, 42.
19 D. Bryce-Smith and A. Gilbert, *Tetrahedron*, 1977, **33**, 2459.
20 M. Bellas, D. Bryce-Smith, M. T. Clarke, A. Gilbert, G. Klunkin, S. Krestonosich, C. Manning and S. Wilson, *J. Chem. Soc., Perkin Trans. 1*, 1977, 2572.
21 H. Shikuza, M. Nakamura and T. Morita, *J. Phys. Chem.*, 1979, **83**, 2019.
22 A. P. de Silva and R. A. D. Dayasin Rupasinghe, *J. Chem. Soc., Chem. Commun.*, 1985, 1669.
23 M. E. Huston and K. W. Haider, *J. Am. Chem. Soc.*, 1988, **110**, 4460.
24 R. A. Bissell, *Top. Curr. Chem.*, 1993, **168**, 223.
25 W. R. Ware, *Pure Appl. Chem.*, 1975, **41**, 635.

Received 24*th August* 1994; *Paper* 4/05187D